Eur. Phys. J. B **60**, 463–468 (2007)
DOI: 10.1140/epjb/e2008-00007-3

The European Physical Journal B

First-principles study of the optical properties of PbFX (X = Cl, Br, I) compounds in its matlockite-type structure

A.H. Reshak[1], Z. Charifi[2,a], and H. Baaziz[2]

[1] Institute of Physical Biology-South Bohemia University, Institute of System Biology and Ecology-Academy of Sciences, Nove Hrady 37333, Czech Republic
[2] Physics Department, Faculty of Science and Engineering, University of M'sila, 28000 M'sila, Algeria

Received 26 March 2007 / Received in final form 4 November 2007

Abstract. We present the results of the *ab initio* theoretical study of the optical properties for PbFX (X = Cl, Br, I) compounds in its matlockite-type structure using the full potential linearized augmented plane wave (FP-LAPW) method as implemented in the WIEN2K code. We employed generalized gradient approximation (GGA), which is based on exchange-correlation energy optimization to calculate the total energy. Also we have used the Engel-Vosko GGA formalism, which optimizes the corresponding potential for band structure calculations. Our calculations show that the valence band maximum (VBM) and conduction band minimum (CBM) are located at Z resulting in a direct energy gap. We present calculations of the frequency-dependent complex dielectric function $\varepsilon(\omega)$ and its zero-frequency limit $\varepsilon_1(0)$. We find that the values of $\varepsilon_1(0)$ increases with decreasing the energy gap. The reflectivity spectra and absorption coefficient has been calculated and compared with the available experimental data. The optical properties are analyzed and the origin of some of the peaks in the spectra is discussed in terms of the calculated electronic structure.

PACS. 61.50.Ks Crystallographic aspects of phase transformations; pressure effects – 71.18.+y Fermi surface: calculations and measurements; effective mass, g factor – 71.15.Mb Density functional theory, local density approximation, gradient and other corrections – 71.15.Nc Total energy and cohesive energy calculations

1 Introduction

Compounds of the PbFCl structure form a large family of interesting host materials for divalent impurities in the case of divalent metal fluoride halides (MFX). These compounds are ionic insulators [1]. The bottom of the conduction bands are formed from the metal atom s and d states and the top of the valence bands arise from the halogen p states with a direct band gap at Z. These compounds when doped with divalent rare-earth ions, Sm^{+2}, are used as a more sensitive pressure gauge than the ruby sensor for high-pressure measurements in a diamond anvil-cell [2]. PbFX (X = Cl, Br, and I) crystals are layered ionic crystals of tetragonal matlockite type [3]. The structure is formed by layers parallel to (001) each occupied by a single kind of ion. The sequence of the layers is F-Pb-X–X-Pb-F where the X layers are doubly occupied with respect to the Pb and F layers [4,5].

Recently Liu et al. [5] investigated the electronic properties of PbFCl by using the pseudopotentiel method in the frame of the generalized gradient approximation (GGA). The reflection, excitation and emission spectra of PbFCl single crystal were also measured using a synchrotron radiation light source in the energy region between 4.0 and 9.5 eV. The absorption and emission of the cation exciton was observed at 5.0 and 3.8 eV, respectively [5]. Haj Hassan et al. [1] have been calculated the structural and electronic properties of the matlockite structure MFX (M = Sr, Ba, Pb; X = Cl, Br, I) compounds by using the full potential linear augmented plane wave method (FP-LAPW).

To the best of our knowledge there is a lack in the experimental data and theoretical calculations of optical properties of these compounds. We would like to mention here there is no full potential theoretical calculation for the optical properties of these compounds has been reported so far. In this paper, we address our selves to report the results concerning the optical properties of PbFX (X = Cl, Br,I) using the full potential calculation.

This paper is organized as follows: In Section 2, we give a brief description of the method used and details of the

---

[a] e-mail: `charifi_z@yahoo.fr`

calculations. In Section 3, results of the optical properties are presented and analysed. Conclusions are drawn in the last section.

2 Details of calculations

We have performed calculations using the full potential linearized augmented plane wave (FP-LAPW) method as incorporated in WIEN2K code [6]. This is an implementation of the density functional theory (DFT) with different possible approximation for the exchange correlation (XC) potentials. The exchange correlation potential was calculated using the generalized gradient approximation (GGA) [7], which is based on exchange-correlation energy optimization to calculate the total energy. Also we have used the Engel-Vosko GGA formalism [8], which optimizes the corresponding potential for band structure calculations.It is well known in the self-consistent band structure calculation within DFT, both LDA and GGA usually underestimate the energy gap [9]. This is mainly due to the fact that they have simple forms that are not sufficiently flexible to accurately reproduce both the exchange correlation energy and its charge derivative. Engel and Vosko considered this shortcoming and constructed a new functional form of GGA [8] which is able to better reproduce the exchange potential at the expense of less agreement in the exchange energy. This approach called EV-GGA, yields better band splitting and some other properties which mainly depend on the accuracy of exchange correlation potential. On the other hand the quantities which depend on an accurate description of E_x, such as the equilibrium volume and bulk modulus are in poor agreement with experiment [9]. For structural properties the exchange-correlation (XC) potential was calculated using the generalized gradient approximation (GGA) in the form proposed by Perdew et al. [7]. For electronic and optical properties we applied the Engel – vosko (EV-GGA) scheme [8].

Kohn-Sham wave functions were expanded in terms of spherical harmonics inside non-overlapping muffin-tin (MT) spheres surrounding the atomic sites and in Fourier series in the interstitial region. Inside the muffin-tin Spheres, the l expansion of the non-spherical potential and charge density were carried out up to $lmax = 10$. The muffin-tin radii were assumed to be 2.0, 2.2, and 2.4 atomic unit (a.u.) for F, Cl, and Br respectively, whereas it is 2.6 a. u. for I and Pb.

PbFX (X = Cl, Br and I) compounds belong to the matlockite structure. This structure is characterized by the tetragonal layered structure which consists of planes perpendicular to the **c**-axis [10]. The space group is P4/nmm (D^7_{4h}, no 129), $Z = 2$. The Pb ions are on one side coordinated by a plane of four fluorine ions and on the other side coordinated by five X ions (X=Cl, Br, I), of which one is on the **c**-axis out of the plane formed by the others. The Pb atoms are located at (0.25, 0.25, ν), (0.75, 0.75,$\overline{\nu}$), the F atoms at (0.75, 0.25, 0), (0.25, 0.75, 0), and X atoms at (0.25, 0.25, u), (0.75, 0.75, $\overline{u}$).

Table 1. The calculated lattice constant, internal parameters, and $\varepsilon_1^{\perp}(0)$ and $\varepsilon_1^{\|}(0)$, compared with the available experimental data.

		Present work	Experimental work
PbFCl	a (A^0)	4.151	4.11 [13]
	c (A^0)	7.354	7.246 [13]
	c/a	1.7716	1.763 [13]
	u	0.6463	0.6497 [13]
	ν	0.2075	0.2058 [13]
	$\varepsilon_1^{\perp}(0)$	4.9	
	$\varepsilon_1^{\|}(0)$	4.5	
PbFBr	a (A^0)	4.232	4.18 [14]
	c (A^0)	7.70	7.59 [14]
	c/a	1.8198	1.816 [14]
	u	0.6469	0.650 [14]
	ν	0.1945	0.195 [14]
	$\varepsilon_1^{\perp}(0)$	5.6	
	$\varepsilon_1^{\|}(0)$	4.9	
PbFI	a (A^0)	4.248	4.23 [14]
	c (A^0)	8.87	8.77 [14]
	c/a	2.088	2.073 [14]
	u	0.6577	0.65 [14]
	ν	0.1665	0.167 [14]
	$\varepsilon_1^{\perp}(0)$	6.8	
	$\varepsilon_1^{\|}(0)$	5.4	

The internal parameters ν and u have been optimized by calculating forces on the nuclei and using the damped Newton Scheme [11] to find equilibrium atomic positions. After relaxation the force on each atom decreases to less than 1.0 mRy/a.u.

We used the optimized internal parameters to calculate the total energy at several volumes around the equilibrium. The results are fitted to the Murnaghan's equation of states [12]. In this way we obtained the equilibrium lattice constant. The calculated lattice constants and internal parameters were used to optimize the c/a ratio of the tetragonal cell with constant volume.

The corresponding equilibrium lattice parameter, c/a ratio and internal parameters obtained within GGA are summarized and compared with experimental data in Table 1. The electronic band structure calculations for these mixed-halide systems, PbFCl, PbFBr, and PbFI have been performed at ambient conditions. The energy band gaps of these compounds have been calculated and compared with the previous theoretical calculations and experimental data, these values are listed in Table 2.

In order to achieve energy eigenvalue convergence, the wave functions in the interstitial region were expanded in plane waves with a cut-off of $Kmax = 8/R_{MT}$ where R_{MT} is the radius of the smallest muffin-tin Sphere. Self-consistency was obtained using 45 k-point in the irreducible Brillouin zone (IBZ), and the BZ integrations were carried out using the tetrahedron method [15]. The anisotropy frequency dependent optical properties are calculated using 470 k-points in the IBZ.

Table 2. The calculated energy band gaps compared with the previous theoretical calculations and the available experimental data.

Eg (eV)	EVGGA[1] LAPW	GGA[1] LAPW	LDA [1] LAPW	GW approximation [5]	Exp [5]	GGA ab initio pseudopotentiel method [5]	This work
PbFCl	4.28	3.49	3.23	5	5.2	3.5	4.32
PbFBr	3.31	2.63	2.39				3.37
PbFI	2.61	1.97	1.73				2.48

3 Optical properties

Since PbFX (X = Cl, Br and I) crystals belong to the tetragonal layered structure we need to calculate two dielectric tensor component to completely characterize the optical properties. Measurement of the dielectric properties is normally done on single crystals. For compounds having tetragonal symmetry, the experiments are performed with electric vector $\vec{E}$ parallel or perpendicular to the **c** axis. The corresponding dielectric functions are $\varepsilon_2^{\perp}(\omega)$ and $\varepsilon_2^{\|}(\omega)$. The calculations of these dielectric function involve the energy eigenvalues and electron wave functions. These are natural outputs of band structure calculations. We have performed calculations of the imaginary part of the interband frequency-dependent dielectric function using the expressions [16]

$$\varepsilon_2^{\|}(\omega) = \frac{12}{m\omega^2} \int_{BZ} \sum_{n,n'} \frac{\left|P_{nn'}^{Z}(k)\right|^2 dS_k}{\nabla\omega_{nn'}(k)}$$

$$\varepsilon_2^{\perp}(\omega) = \frac{6}{m\omega^2} \int_{BZ} \sum_{n,n'} \frac{\left[\left|P_{nn'}^{X}(k)\right|^2 + \left|P_{nn'}^{Y}(k)\right|^2\right] dS_k}{\nabla\omega_{nn'}(k)}.$$

The above expressions are written in atomic units with $e^2 = 1/m = 2$ and $\hbar = 1$. where ω is the photon energy. $P_{nn'}^{X}(k)$ and $P_{nn'}^{Z}(k)$ are the X and Z component of the dipolar matrix elements between initial $|nk\rangle$ and final $|n'k\rangle$ states with their eigenvalues $\mathrm{E}_n(k)$ and $\mathrm{E}_{n'}(k)$, respectively. $\omega_{nn'}(k)$ is the energy difference $\omega_{nn'}(k) = \mathrm{E}_n(k) - \mathrm{E}_{n'}(k)$ and S_k is a constant energy surface $S_{k=}\{k;\ \omega_{nn'}(k) = \omega\}$. The integral is over the first Brillouin zone.

The real parts $\varepsilon_1^{\perp}(\omega)$ and $\varepsilon_1^{\|}(\omega)$ of the frequency dependent dielectric function can be derived from the imaginary part using the Kramers–Kronig relations [17]. The reflectivity $R(\omega)$, the absorption coefficient $I(\omega)$, refractive index $n(\omega)$, and extinction coefficient $k(\omega)$ in the crystal are related to the reflectivity at normal incidence by [17]

$$R^{\perp}(\omega) = \frac{n^{\perp}(\omega) + ik^{\perp}(\omega) - 1}{n^{\perp}(\omega) + ik^{\perp}(\omega) + 1}$$

$$I^{\perp}(\omega) = \sqrt{2}\omega \left[\sqrt{\varepsilon_1^{\perp}(\omega)^2 + \varepsilon_2^{\perp}(\omega)^2} - \varepsilon_1^{\perp}(\omega)\right]^{1/2}$$

$$k^{\perp}(\omega) = I^{\perp}(\omega)/2\omega$$

$$n^{\perp}(\omega) = \left(1\big/\sqrt{2}\right) \left[\sqrt{\varepsilon_1^{\perp}(\omega)^2 + \varepsilon_2^{\perp}(\omega)^2} + \varepsilon_1^{\perp}(\omega)\right]^{1/2}.$$

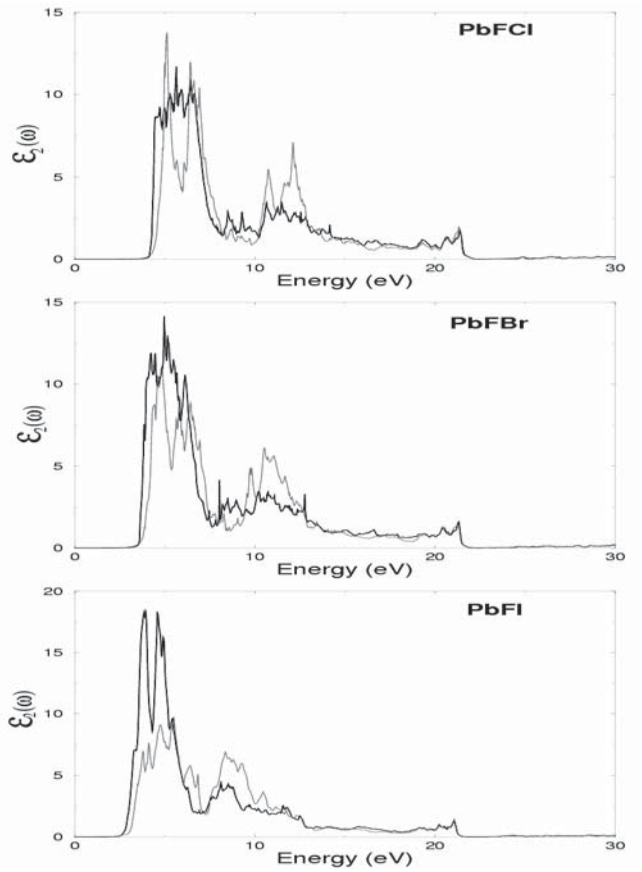

Fig. 1. Calculated $\varepsilon_2^{\perp}(\omega)$ (dark curve) and $\varepsilon_2^{\|}(\omega)$ (light curve) for PbFX compounds.

With similar expressions for the parallel component. In the calculations of the optical properties, a dense mesh of uniformly distributed k-points is required. Hence, the Brillouin zone integration was performed with 470 k-points in the irreducible part of the Brillouin zone.

Figure 1, displays $\varepsilon_2^{\perp}(\omega)$ and $\varepsilon_2^{\|}(\omega)$ for the investigated compounds for a radiation up to 30 eV. Half-width broadening is taken to be 0.01 eV. As can be seen the linear optical absorption varies from one compound to another. This is attributed to the fact that the conduction bands are different, and the symmetries of the wave functions dictate that the selection rules are fully reflected in the Matrix Moment Elements (MME's).

It would be useful to identify the transitions that are responsible for the spectral structures in $\varepsilon_2^{\perp}(\omega)$ and $\varepsilon_2^{\|}(\omega)$ using our calculated band structure. In order to identify

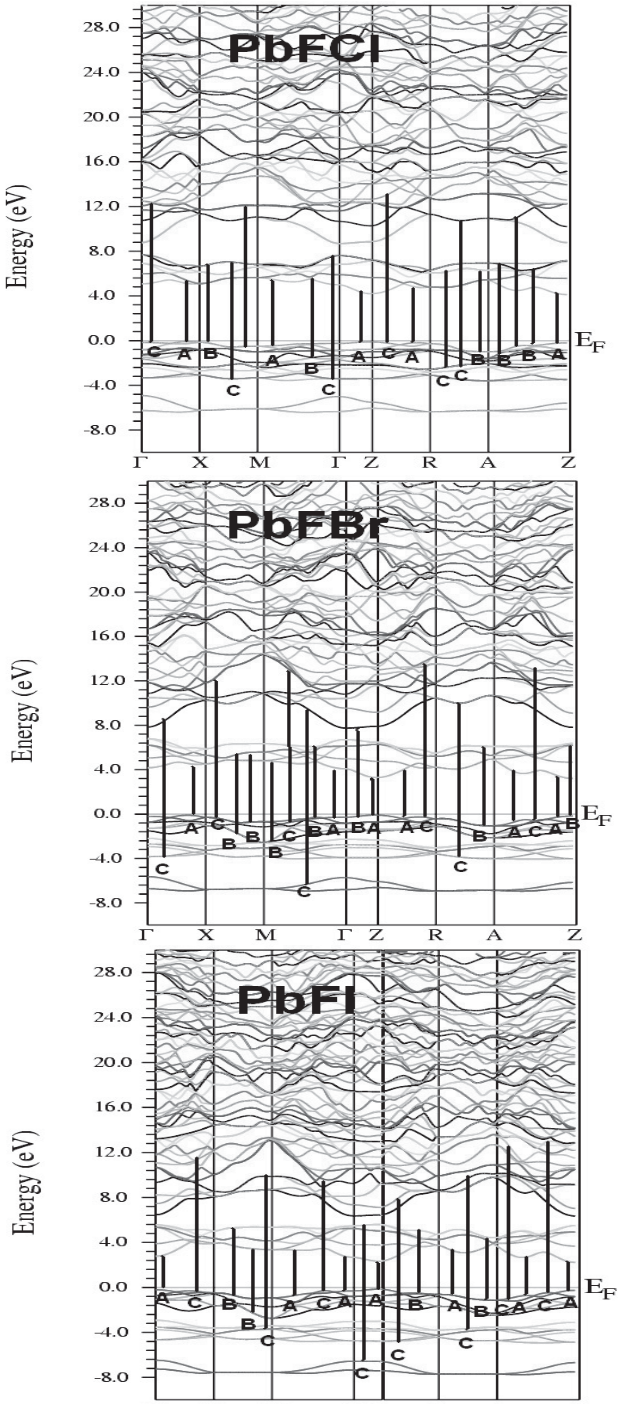

Fig. 2. The optical transitions depicted on a generic band structure.

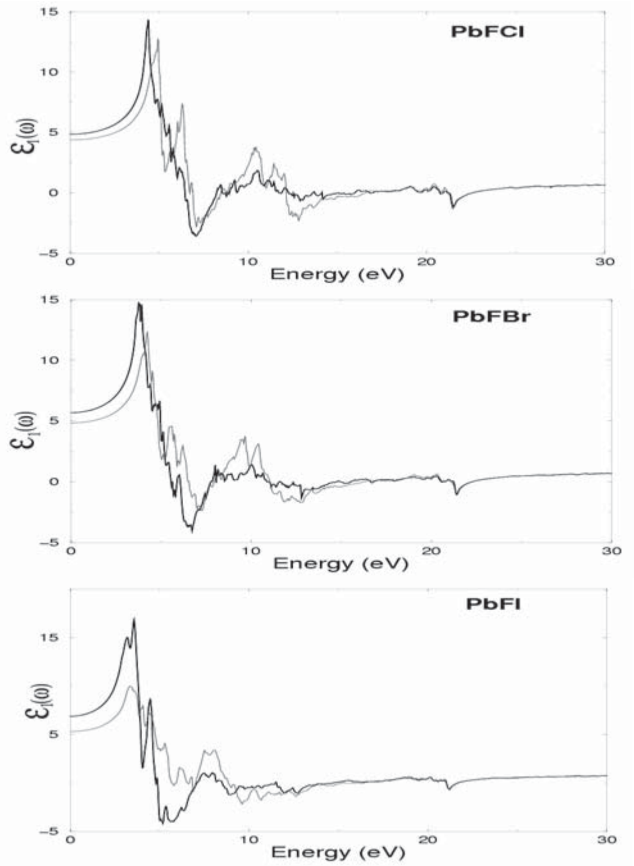

Fig. 3. Calculated $\varepsilon_1^{\perp}(\omega)$ (dark curve) and $\varepsilon_1^{\parallel}(\omega)$ (light curve) for PbFX compounds.

these structures we need to look at the magnitude of the optical matrix elements. The observed structures would correspond to those transitions which have large optical matrix elements. We have indicated these transitions in the band structure diagram. These transitions are labeled according to the peak positions in Figure 1. For simplicity we have labeled the transitions in Figure 2 as A (0–5) eV, B (5–7) eV, and C (7–12) eV. The peaks in the optical response are caused by the electric-dipole transitions between the valence and conduction bands. From Figure 1, it can also be seen that the edge of optical absorption for $\varepsilon_2^{\perp}(\omega)$ is located at 4.32, 3.37 and 2.48 eV for PbFX (X = Cl, Br, I) respectively. These points are Z_{v}–Z_c splitting which gives the threshold for direct optical transitions between the highest valence band and the lowest conduction band. This is known as the fundamental absorption edge. These critical points are followed by small structure localized at 12.5, 11.5, and 9.0 eV and the main peaks in the spectra are situated at 7.0, 6.0, and 5.0 eV for PbFCl, PbFBr, PbFI, respectively.

According to the Kramers-Kronig dispersion relation the real part $\varepsilon_1^{\perp}(\omega)$ and $\varepsilon_1^{\parallel}(\omega)$ of the frequency dependent dielectric function $\varepsilon(\omega)$ is also obtained and displayed in Figure 3. We note that PbFI show the highest peak intensity in these spectra. The main peaks are located at about 4.5, 4.0 and 3.5 eV for PbFCl, PbFBr, and PbFI respectively. The main peak is followed by a hump between 7.5–13.5, 7.0–13.0, and 6.0–10.0 eV. For all the investigated compounds $\varepsilon_1(\omega)$ goes to be negative at about 7.0, 6.0, and 5.0 eV, then oscillating around zero.

The static dielectric constant $\varepsilon_1(0)$ is given by the low energy limit of $\varepsilon_1(\omega)$. Note that we do not include phonon contributions to the dielectric screening, and $\varepsilon_1(0)$ corresponds to the static optical dielectric constant ε_∞. Our

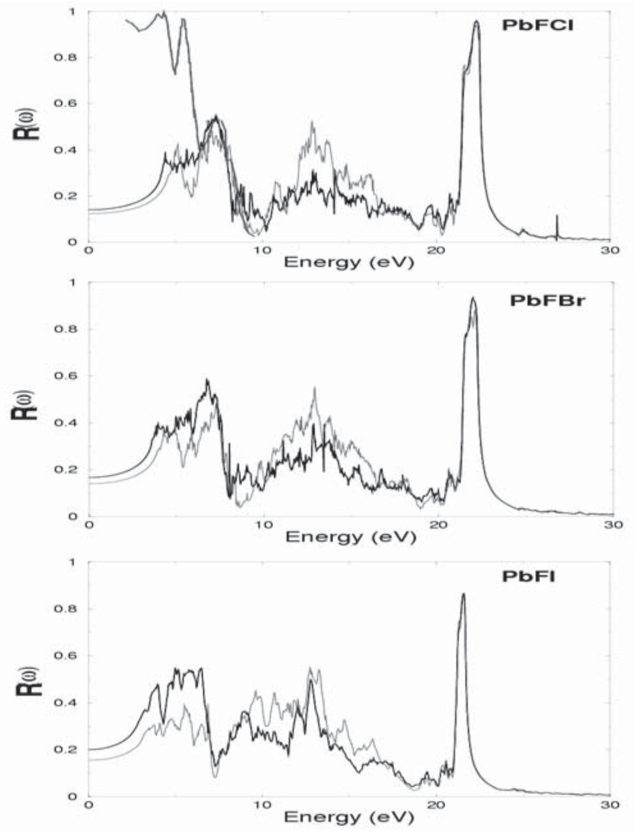

Fig. 4. Calculated $R^{\perp}(\omega)$ (dark curve) and $R^{\parallel}(\omega)$ (light curve), along with the experimental data (thick light curve) of Liu et al. [5] for PbFCl compound.

calculated optical dielectric constants $\varepsilon_{\infty}$are listed in Table 1. We find that the values of $\varepsilon_1^{\perp}(0)$ and $\varepsilon_1^{\parallel}(0)$ increases with decreasing the energy gap. This could be explained on the basis of the Penn model [18]. Penn model is based on the expression$\varepsilon(0) \approx 1 + (\hbar\omega_P/E_g)^2$. It is clear that $\varepsilon(0)$ is inversely proportional with E_g. Hence smaller E_g yields larger $\varepsilon(0)$. We can determine E_g from this expression by using the values of $\varepsilon(0)$ and the plasma energy $\hbar\omega_P$.

In Figures 4 the reflectivity spectrum $R^{\perp}(\omega)$ and $R^{\parallel}(\omega)$ are plotted and compared with the available experimental data [5]. Our calculation shows very good agreement with the available experimental data especially at the energy range between 5.0–9.5 eV, while it shows poor agreement at the low energies less than 5.0 eV. From the reflectivity spectra of these compounds, we note that at low energies $R^{\perp}(\omega)$ and $R^{\parallel}(\omega)$ increases up to about 60% forming a strong reflectivity maximum between 1.0–10 eV arises from inter-band transitions. Very sharp decreasing forms a strong reflectivity minimum at energies ranging between 7.5–11.0 eV indicating a collective plasma resonance. The depth of the plasma minimum is determined by the imaginary part of the dielectric function at the plasma resonance and is representative of the degree of overlap between the inter-band absorption regions. At the higher energies the spectrum shows very high reflectivity.

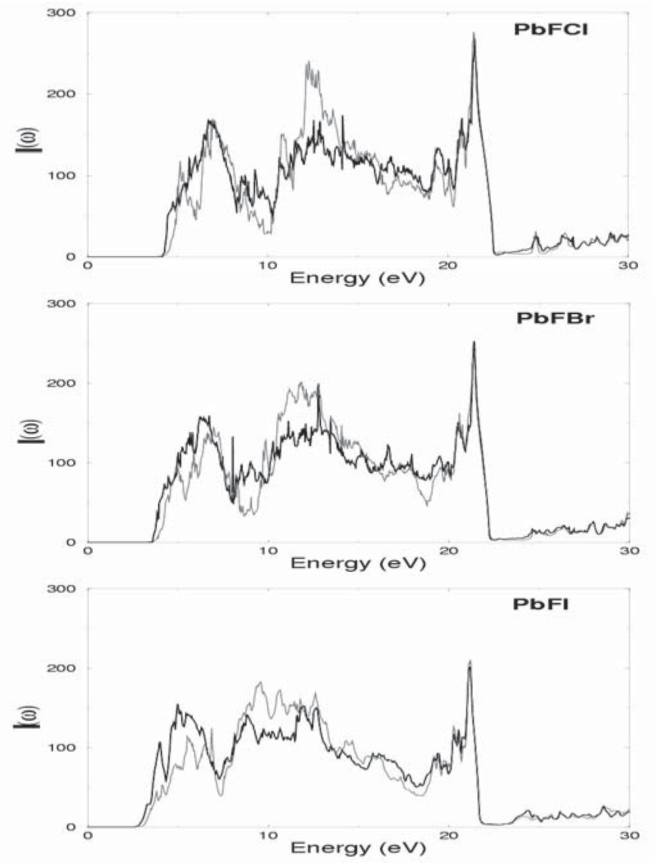

Fig. 5. Calculated $I^{\perp}(\omega)$ (dark curve) and $I^{\parallel}(\omega)$ (light curve) for PbFX compounds.

Figure 5 shows the absorption coefficient $I^{\perp}(\omega)$ and $I^{\parallel}(\omega)$ for the investigated compounds. We again find three main structures. These materials possess considerable absorption. Our calculated reflectivity and absorption coefficient shows considerable anisotropy at low energies.

We note that the all frequency-dependent optical properties of these compounds are shifted towards lower energies when we move from PbFCl to PbFBr, to PbFI. That is attributed to the fact that the bandwidth of the conduction bands increases with subtracting Cl by Br by I.

4 Conclusions

We have performed calculations of the frequency dependent optical properties for the PbFX (X = Cl, Br, I) compounds, using the FP-LAPW method. Our calculations show that these compounds has direct energy band gap. We present calculations of the frequency-dependent complex dielectric function $\varepsilon(\omega)$. Also we calculate the values of $\varepsilon_1^{\perp}(0)$ and $\varepsilon_1^{\parallel}(0)$. We find that the values of $\varepsilon_1^{\perp}(0)$ and $\varepsilon_1^{\parallel}(0)$ increases with decreasing the energy gap. This could be explained on the basis of the Penn model. We used our calculated band structures to analyze the optical transitions. The reflectivity spectra and absorption coefficient has been calculated. We compared our calculated reflectivity with the available experimental data of Liu et al. [5]. Our calculated reflectivity shows poor agreement with the available experimental data at the low energies less than 5.0 eV, while it shows very good agreement at the energy range between 5.0–9.5 eV. A considerable anisotropy is found between the parallel and perpendicular components of the frequency-dependent optical properties. To the best of our knowledge, there is no full potential theoretical calculation for the optical properties of these compounds has been reported so far. We believe that our calculations could be useful to cover the lack of data for these compounds. In order to make more detail comparison with the experimental data we have calculated the frequency-dependent reflectivity. Also we have calculated the absorption coefficient of these compounds.

This work was supported from the institutional research concept of the Institute of Physical Biology, UFB (No. MSM6007665808), and the Institute of System Biology and Ecology, ASCR (No. AVOZ60870520).

References

1. F.El. Haj Hassan, H. Akbarzadeh, S.J. Hashemifar, A. Mokhtari, J. Phys. Chem. Solids **65**, 1871 (2004)
2. G. Kalpana, B. Palanivel, I.B. Shameem Banu, M. Rajagopalan, Phys. Rev. B **56**, 3532 (1997)
3. R.W. Wyckoff, *Crystal structure* (Interscience, New York, 1948)
4. M. Mérawa, Y. Noël, B. Civalleri, R. Brown, R. Dovesi, J. Phys: Condens. Matter **17**, 535 (2005)
5. B. Liu, C. Shi, M. Yin, Y. Fu, D. Shen, J. Phys: Condens. Matter **17**, 5087 (2005).
6. P. Blaha, K. Schwarz, G.K.H. Madsen, D. Kvasnicka, J. luitz, *WIEN2K, "an Augmented Plane Wave + Local orbitals program for calculating crystal properties"*, Karlheinz Schwarz, Techn. Universitat, Wien, Austria, 2001, ISBN 3-9501031-1-2
7. J.P. Perdew, S. Burke, M. Ernzerhof, Phys. Rev. Lett. **77**, 3865 (1996)
8. E. Engel, S.H. Vosko, Phys. Rev. B **47**, 13164 (1993)
9. P. Dufek, P. Blaha, K. Schwarz, Phys. Rev. B **50**, 7279 (1994)
10. H.P. Beck, Z. Anorg, Allg. Chem. **451**, 73 (1979)
11. B. Koher, S. Wilke, M. Scheffler, R. Kouba, C. Ambrosch-Draxl, Comput. Phys. Comm. **94**, 319 (1996)
12. F.D. Murnaghan, Proc. Natl. Acad. Sci. USA **30**, 244 (1944)
13. M. Pasero, N. Perchiazzi, Miner. Mag. **60**, 833 (1996)
14. NBS, Mongr 25, Sec. **10**, 26 (1972); 25, Sec. **13**, 25 (1976)
15. O. Jepsen, O.K. Andersen, Solid State Commun. **9**, 1763 (1971)
16. S. Hufner, R. Claessen, F. Reinert, Th. Straub, V.N. Strocov, P. Steiner, J. Electron Spectrosc. Relat. Phenom. **100**, 191 (1999); R. Ahuja, S. Auluck, B. Johansson, M.A. Kan, Phys. Rev. B **50**, 2128 (1994)
17. F. Wooten, *Optical Properties of Soilds* (Academic, New York, 1972)
18. D.R. Penn, Phys. Rev. **128**, 2093 (1962)